Macromolecular Journals

Macromolecular Theory and Simulations

Phase Behavior of Amphiphilic Molecules in the Presence of One Solvent: A Dissipative Particle Dynamics Study

Ching-I Huang,* Hsiao-Yang Hsueh, Yi-Kang Lan, Yu-Chih Lin

We simulate the phase behavior of amphiphilic molecules in the presence of one solvent by DPD. In general, DPD has successfully captured most of the effects of composition of amphiphilic molecules, solvent selectivity, and solvent amount, on the phase transition behavior obtained by both SCMF calculations and experiments. When a neutral good solvent is added, the solutions undergo a lyotropic transition analogous to the thermotropic transition in the melts. Furthermore, the order-disorder transition results obtained via DPD are in good agreement with theoretical predictions by including the fluctuation effects, as well as with experiments. In the selective solvents, various transitions from the "normal" phases (i.e., the minority blocks form the minor domains) to even the "inverted" phases (formed by the majority blocks) have been observed by varying solvent selectivity and solvent amount. Since the packing order of the spheres is greatly affected by the finite size of the simulation box, it becomes difficult to examine the most stable packing array of spheres via DPD as has been predicted by SCMF theory. However, DPD reveals a possible spherical order of A15, which has been ignored in current SCMF work but observed in some amphiphilic molecule systems.

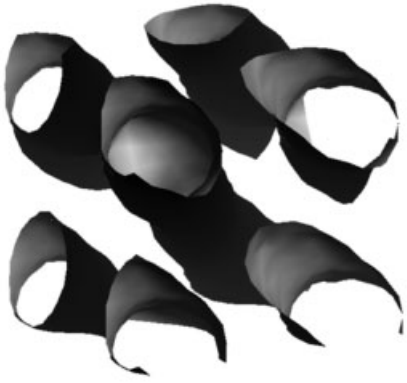

Introduction

Amphiphilic molecules, such as surfactants, lipids, and block copolymers, continue to attract a lot of attention due to the fact that they can self-assemble into a rich variety of morphologies.[1–6] Many of the amphiphilic molecule systems with valuable technological applications are associated with the addition of one solvent. By varying the composition of amphiphilic molecules, solvent amount, and solvent selectivity, it is possible to obtain a variety of microstructures.

When a neutral solvent S (i.e., the interaction parameters $\chi_{AS} = \chi_{BS}$) is added to an AB amphiphilic molecule, provided the concentrated regime and the solvent quality is good, the solutions at a volume fraction of amphiphilic molecules ϕ behave as a neat system with the effective A/B interaction parameter simply equal to $\phi\chi_{AB}N$, which is named the "dilution approximation".[7] Previous self-consistent mean-field (SCMF) calculations have shown that the equilibrium solution phase maps are almost identical to the melt phase map by replacing $\chi_{AB}N$ with

C.-I Huang, H.-Y. Hsueh, Y.-K. Lan, Y.-C. Lin
Institute of Polymer Science and Engineering, National Taiwan University, Taipei 106, Taiwan
Fax: +886 2 3366 5237; E-mail: chingih@ntu.edu.tw

InterScience

DOI: 10.1002/mats.200600057

$\phi\chi_{AB}N$.[8–11] That is, as in the melts, the composition of amphiphilic molecules f largely determines the geometry of the microstructure, in which the shorter blocks form the minor domains. These SCMF results have been confirmed experimentally in predicting the order-order transitions (OOTs).[12–14] While even for the concentrated solutions the order-disorder transition (ODT) instead follows the prediction by both Olvera de la Cruz[15] and Fredrickson and Leibler:[16] $(\phi^{1.59}\chi_{AB}N)_{ODT} = F(f)$, as given in the melts.[12–14,17] When a selective solvent is added (i.e., $\chi_{AS} \neq \chi_{BS}$), the shape and the packing symmetry of the ordered structure is determined not only by the composition f but also by the solvent selectivity. There have been a great deal of experimental[12,13,18–31] and theoretical[11,32–34] studies on the resulting phase behavior. In contrast to the neat diblock copolymer microstructures, the amphiphilic molecule solutions may form the "inverted" phases, where the longer blocks form the minor domains, by varying solvent selectivity and ϕ. Furthermore, unlike the melts where the "normal" spheres (i.e., formed by the minority blocks) adopt the body-centered cubic (bcc) array, the spherical packing order in amphiphilic molecule solutions is strongly dependent on solvent selectivity and ϕ. Our previous SCMF theoretical results[34] have shown that upon adding a selective solvent for the minority blocks so that the "inverted" spheres are formed by the majority blocks, a more dense face-centered cubic (fcc) packing order is favored over bcc with increasing the solvent selectivity and/or solvent amount.

Just as described above, most of the theoretical phase behavior studies of amphiphilic molecule solutions are based on the SCMF theory, in which to determine the equilibrium microstructure one has to compare the free energies of different possible phases. Recently a relatively new and direct simulation method known as dissipative particle dynamics (DPD)[35] has been developed and successfully applied to study the mesophase behavior for a variety of amphiphilic molecule systems.[36–45] Groot and Madden first applied DPD to examine the microphase separation behavior of linear A_mB_n diblock copolymer melts.[37] The phase diagram they constructed in terms of the A composition and the effective A/B segregation parameter is in near quantitative agreement with that predicted by the SCMF theory.[46] In the amphiphilic molecule solutions, the related current DPD studies were mainly focused on the less concentrated regimes.[38–41,43,45] For example, Cao et al.[45] employed DPD to simulate the aggregation behavior of poly(ethylene oxide)-poly(propylene oxide) block copolymers in aqueous solutions. In particular, the effects of the copolymer architecture and concentration on the formed micelle type and size were examined. Though these solution studies demonstrated that the DPD simulation method is an appropriate technique to examine the phase behavior of amphiphilic molecules in dilute solutions, the effects of a solvent addition on the resulting microstructure formation of amphiphilic molecules in the concentrated regimes have not been fully examined by DPD.

In this paper, we thus aim to simulate the phase behavior for an AB type of amphiphilic molecule in the presence of one solvent (S) by the DPD simulation method. We focus on whether DPD can qualitatively capture the effects of composition of amphiphilic molecules, solvent amount, and solvent selectivity, on the resulting microphase separation behavior in the amphiphilic molecule solutions as obtained by SCMF calculations and experiments. For simplicity, we assume that each component has the same volume per segment (bead). We choose A_mB_n to resemble the amphiphilic molecules, where $m+n=10$, and vary the A composition $f=m/(m+n)$. The solvent S is characterized by a bead. Hence, our present simulated system via DPD with the ratio of degree of polymerization $N_S/N_{AB}=1/10$, corresponds to short amphiphilic molecules in the presence of a solvent. Note that most of the current phase behavior studies by the SCMF theory and experiments are focused on very long amphiphilic molecules (i.e., diblock copolymers) with respect to the solvent size. One may ask: why not simulate the same systems as in the previous SCMF calculations. This is simply due to the fact that the phase behavior has to be simulated in a very large box, which becomes too time-consuming and impractical. As such, a quantitative comparison between the phase behavior predicted by SCMF and DPD is impossible to reach in our current study. Instead, we only focus on the qualitative validation of the DPD simulation method applied to the phase behavior of amphiphilic molecule solutions from concentrated to less concentrated regimes.

The DPD Simulation Method

In a DPD simulation, the time evolution of motion for a set of interacting particles is solved by Newton's equation. For simplicity, we assume that the masses of all particles are equal to 1. The force acting on the i-th particle $\vec{f}_i$ contains three parts: a conservative force $\vec{F}_{ij}^{C}$, a dissipative force $\vec{F}_{ij}^{D}$, and a random force $\vec{F}_{ij}^{R}$, that is,

$$\vec{f}_i = \sum_{i \neq j} \left(\vec{F}_{ij}^{C} + \vec{F}_{ij}^{D} + \vec{F}_{ij}^{R} \right) \quad (1)$$

where the sum is over all other particles within a certain cut-off radius r_c. As this short-range cut-off counts only local interactions, r_c is usually set to 1 so that all lengths are measured relative to the particle radius.

Macromol. Theory Simul. 2007, 16, 77–85

Macromolecular Journals
DOI: 10.1002/mats.200600057

The conservative force $\vec{F}_{ij}^{C}$ is a soft repulsive force and given by,

$$\vec{F}_{ij}^{C} = \begin{cases} a_{ij}\left(1 - \frac{r_{ij}}{r_c}\right)\vec{n}_{ij} & r_{ij} < r_c \\ 0 & r_{ij} \geq r_c \end{cases} \quad (2)$$

where a_{ij} is the repulsive interaction parameter between particles i and j, $\vec{r}_{ij} = \vec{r}_i - \vec{r}_j$, $r_{ij} = |\vec{r}_{ij}|$, and $\vec{n}_{ij} = \frac{\vec{r}_{ij}}{r_{ij}}$. The repulsion parameter a_{ij} is often related to the Flory-Huggins interaction parameter χ_{ij} by the following equation,[36]

$$\begin{aligned} a_{ij}(T) &= a_{ii} + 3.497 k_B T \chi_{ij}(T) \quad \text{for} \quad \rho = 3 \\ a_{ij}(T) &= a_{ii} + 1.451 k_B T \chi_{ij}(T) \quad \text{for} \quad \rho = 5 \end{aligned} \quad (3)$$

where ρ is the particle density of the system. The term a_{ii}, which corresponds to the repulsion parameter between particles of the same type, i, is determined by matching the water compressibility as,[36]

$$a_{ii} = 75 k_B T/\rho \quad (4)$$

The dissipative force $\vec{F}_{ij}^{D}$ is a hydrodynamic drag force and given by,

$$F_{ij}^{D} = \begin{cases} -\gamma \omega^{D}(r_{ij})(\vec{n}_{ij} \cdot \vec{v}_{ij})\vec{n}_{ij} & r_{ij} < r_c \\ 0 & r_{ij} \geq r_c \end{cases} \quad (5)$$

where γ is a friction parameter, ω^{D} is an r-dependent weight function vanishing for $r \geq r_c$, and $\vec{v}_{ij} = \vec{v}_i - \vec{v}_j$.

The random force $\vec{F}_{ij}^{R}$ corresponds to the thermal noise and has the form of,

$$\vec{F}_{ij}^{R} = \begin{cases} \sigma \omega^{R}(r_{ij})\theta_{ij}\vec{n}_{ij} & r_{ij} < r_c \\ 0 & r_{ij} \geq r_c \end{cases} \quad (6)$$

where σ is a parameter, ω^{R} is also a weight function and $\theta_{ij}(t)$ is a randomly fluctuating variable. Note that these two forces, $\vec{F}_{ij}^{D}$ and $\vec{F}_{ij}^{R}$, also act along the line of centers and conserve linear and angular momentum. There is an independent random function for each pair of particles. Also there is a relation between both constants γ and σ as follows,[36]

$$\sigma^2 = 2\gamma k_B T \quad (7)$$

In our simulations, $\gamma = 4.5$ and the temperature $k_B T = 1$. As such, $\sigma = 3.0$ according to Equation (7).

In order for the steady-state solution to the equation of motion to be the Gibbs ensemble and for the fluctuation-dissipation theorem to be satisfied, it has been shown that only one of the two weight functions $\omega^{D}$and ω^{R} can be chosen arbitrarily,[47]

$$\omega^{D}(r) = [\omega^{R}(r)]^2 \quad (8)$$

which, furthermore, is usually taken as,

$$\omega^{D}(r) = [\omega^{R}(r)]^2 = \begin{cases} (r_c - r_{ij})^2 & r_{ij} < r_c \\ 0 & r_{ij} \geq r_c \end{cases} \quad (9)$$

Finally, the spring force $\vec{f}^{S}$, which acts between the connected beads in a molecule, has the form of,

$$\vec{f}_i^{S} = \sum_j C\vec{r}_{ij} \quad (10)$$

where C is a harmonic type spring constant for the connecting pairs of beads in a molecule, and is chosen equal to 4 (in terms of $k_B T$).[36]

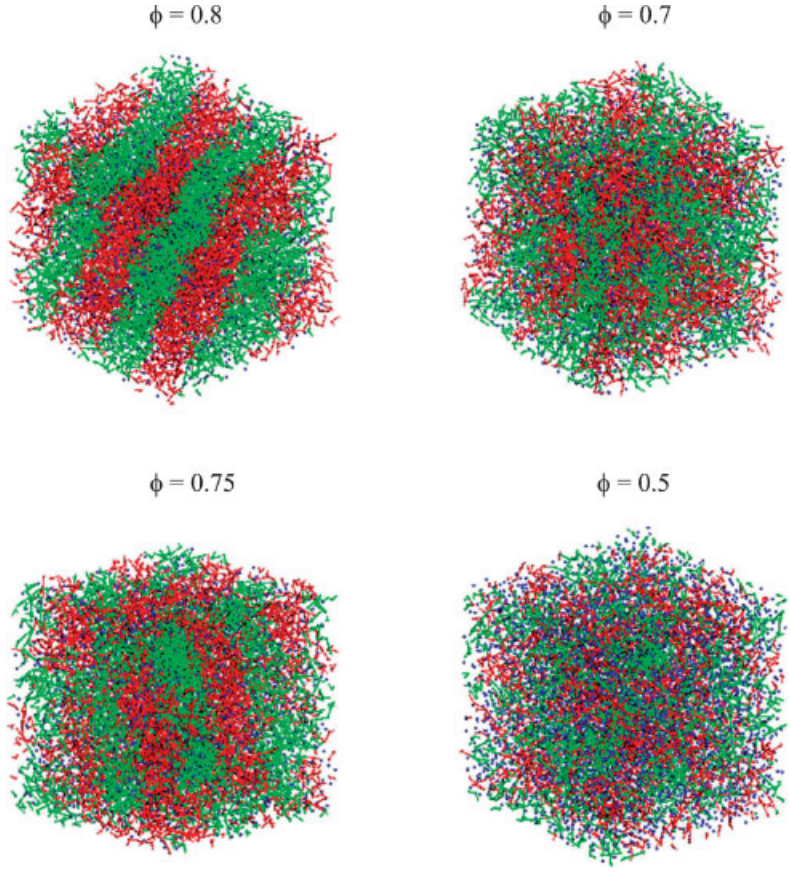

Figure 1. Morphology variation of A_5B_5 in the presence of a neutral solvent S with ϕ, simulated in a box of $15 \times 15 \times 15$. The interaction parameters are set as $a_{AB} = 40$ and $a_{AS} = a_{BS} = 25$. The red, green, and blue colors represent A, B, and S, respectively.

Note that a modified version of the velocity Verlet algorithm is used here to solve the Newtonian equation of motion,[48]

$$r_i(t+\Delta t) = r_i(t) + v_i(t)\cdot\Delta t + \frac{1}{2}f_i(t)\cdot\Delta t^2$$
$$\tilde{v}_i(t+\Delta t) = v_i(t) + \lambda f_i(t)\cdot\Delta t$$
$$f_i(t+\Delta t) = f_i[r_i(t+\Delta t) + \tilde{v}_i(t+\Delta t)]$$
$$v_i(t+\Delta t) = v_i(t) + \frac{1}{2}\Delta t\cdot[f_i(t) + f_i(t+\Delta t)] \quad (11)$$

In particular, we choose $\lambda = 0.65$ and $\Delta t = 0.05$ here. As such, the time evolution of morphology patterns is recorded until the systems show a stable pattern.

Results and Discussion

In simulating the phase separation behavior of A_mB_n amphiphilic molecules in the presence of a solvent S by DPD, the particle density ρ is kept equal to 3. As such, the dimensionless repulsion parameter (i.e., in terms of k_BT) between equal particles a_{ii} in Equation (4) is set equal to 25 to resemble the Flory interaction parameters $\chi_{II} = 0$; I = A, B, S. We adopt a 3-D lattice with at least $15 \times 15 \times 15$ grids to assure that the side length of our simulation box is significantly larger than the radius of gyration of amphiphilic molecules. The value of the radius of gyration for A_mB_n with $m+n=10$ simulated here is around 1.2–1.4 grids. In each pattern, the red, green, and blue colors correspond to component A, B, and S, respectively.

We first examine the effects of a neutral solvent on the phase behavior of amphiphilic molecules. Figure 1 displays the structural patterns at various ϕ for A_5B_5 in the presence of a neutral solvent when $a_{AB} = 40$ and $a_{AS} = a_{BS} = 25$. According to Equation (3), the parameter $a_{AB} = 40$ corresponds to $\chi_{AB} = 4.3$. Therefore, the effective A/B interaction parameter $(\chi_{AB}N)_{eff}$ calculated by the following equation,[37,42]

$$(\chi_{AB}N)_{eff} = \frac{\chi_{AB}N}{1 + 3.9N^{\frac{2}{3}-2\nu}} \quad (12)$$

is equal to 15.3 and 19.5 for unperturbed Gaussian chains (i.e., $\nu = 0.5$) and swollen chains ($\nu = 0.588$), respectively. No matter which value of $(\chi_{AB}N)_{eff}$ is used, according to the prediction by the SCMF theory,[46] A_5B_5 forms the stable lamellar (L) phase, as expected. With adding the solvent amount (i.e., decreasing ϕ), it is clear that the solutions with $\phi \geq 0.75$ form a well ordered lamellar (L) phase and become disordered (D) as $\phi \leq 0.5$. This is not surprising since the dilution of a neutral good solvent to symmetric lamellar amphiphilic molecules is analogous to reducing the effective segregation between A and B. Note that between the totally disordered and the well ordered L phase, for example when $\phi = 0.7$, the corresponding pattern in Figure 1 shows a micelle-like structure, that is with chains aggregating as large droplets but no formation of well ordered structures. If we sort it out as the disordered state, the order disorder transition ϕ_{ODT} from the DPD simulations occurs between 0.7 and 0.75. With the corresponding value of $(\chi_{AB}N)_{eff} = 15.3$ for Gaussian chains ($\nu = 0.5$) and 19.5 for swollen chains ($\nu = 0.588$), ϕ_{ODT} predicted by the dilution approximation of SCMF theory[7] ranges between 0.69 and 0.54; while ϕ_{ODT} by including the fluctuation effects[15,16] are 0.79 and 0.68. It is clear that our simulation results for amphiphilic molecules in a neutral solvent by DPD are in a better agreement with the theoretical predictions by including the fluctuation effects.

Figure 2 presents the phase map in terms of the A composition f and ϕ for an amphiphilic molecule A_mB_n ($m+n=10$) in the presence of a B-selective solvent S with interaction parameters $a_{AS} = 50$, $a_{BS} = 25$, and $a_{AB} = 50$. When the solutions are concentrated, as f decreases from 0.5, a transition of lamellae (L) → perforated A-layers (PL_A) or gyroid (G_A) → hexagonally-packed A-formed cylinders (C_A^{HEX}) → ordered A-formed spheres (S_A) → disordered micelles ($D^{micelle}$) → disordered phase (D) is observed. That is, the morphology is mainly dominated by the composition f, similar to that in the amphiphilic copolymer melts. As the solutions becomes less concentrated, due to the fact that S prefers the B block and thus acts in a

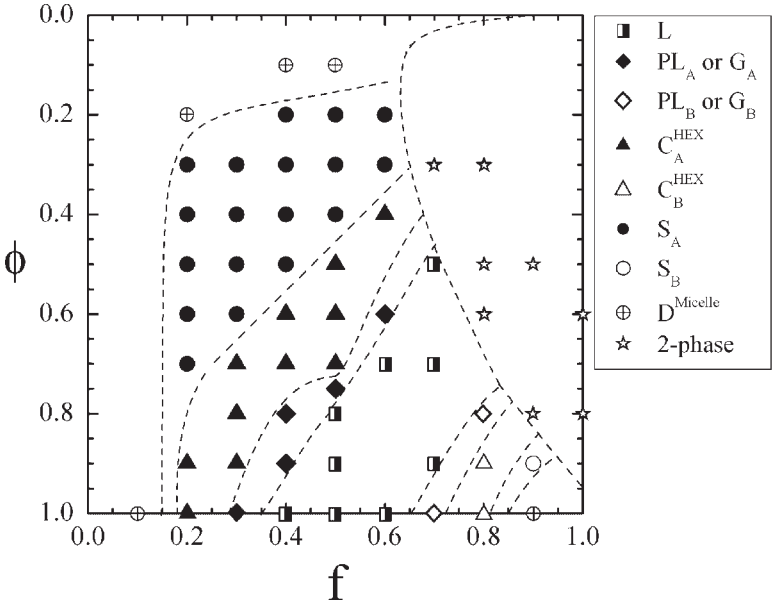

Figure 2. Two-dimensional phase map as a function of f and ϕ for A_mB_n ($m+n=10$) in the presence of a selective solvent S with interaction parameters $a_{AS} = 50$, $a_{BS} = 25$, and $a_{AB} = 50$.

Macromol. Theory Simul. **2007**, *16*, 77–85

Macromolecular Journals
DOI: 10.1002/mats.200600057

manner that corresponds qualitatively to reducing the A composition, the formation of A-formed cylinders as well as spheres is expected even for $f \geq 0.5$. In Figure 3 we present the corresponding patterns at various ϕ for A_5B_5 in the B-selective solvent S when $a_{AS} = 50$, $a_{BS} = 25$, and $a_{AB} = 50$. As expected, S distributes more in the B-rich domains, and a transition of L $(\phi \geq 0.8) \rightarrow PL_A$ $(\phi = 0.75) \rightarrow C_A^{HEX}$ $(0.7 \geq \phi \geq 0.5) \rightarrow S_A^{FCC}$ $(0.4 \geq \phi \geq 0.2) \rightarrow$ $D^{micelle}$ $(\phi = 0.1) \rightarrow$ D occurs as ϕ decreases. In addition to the various microphase transitions induced by varying ϕ, a macrophase separation into an AB molecule-rich and an S-rich phase occurs when $f > 0.5$ due to the immiscibility between A and S. As can be seen in Figure 4, where the structural patterns at various ϕ for A_8B_2 $(f = 0.8)$ in the B-selective solvent S $(a_{AS} = 50$, $a_{BS} = 25)$ and $a_{AB} = 50$ are shown, a lyotropic transition

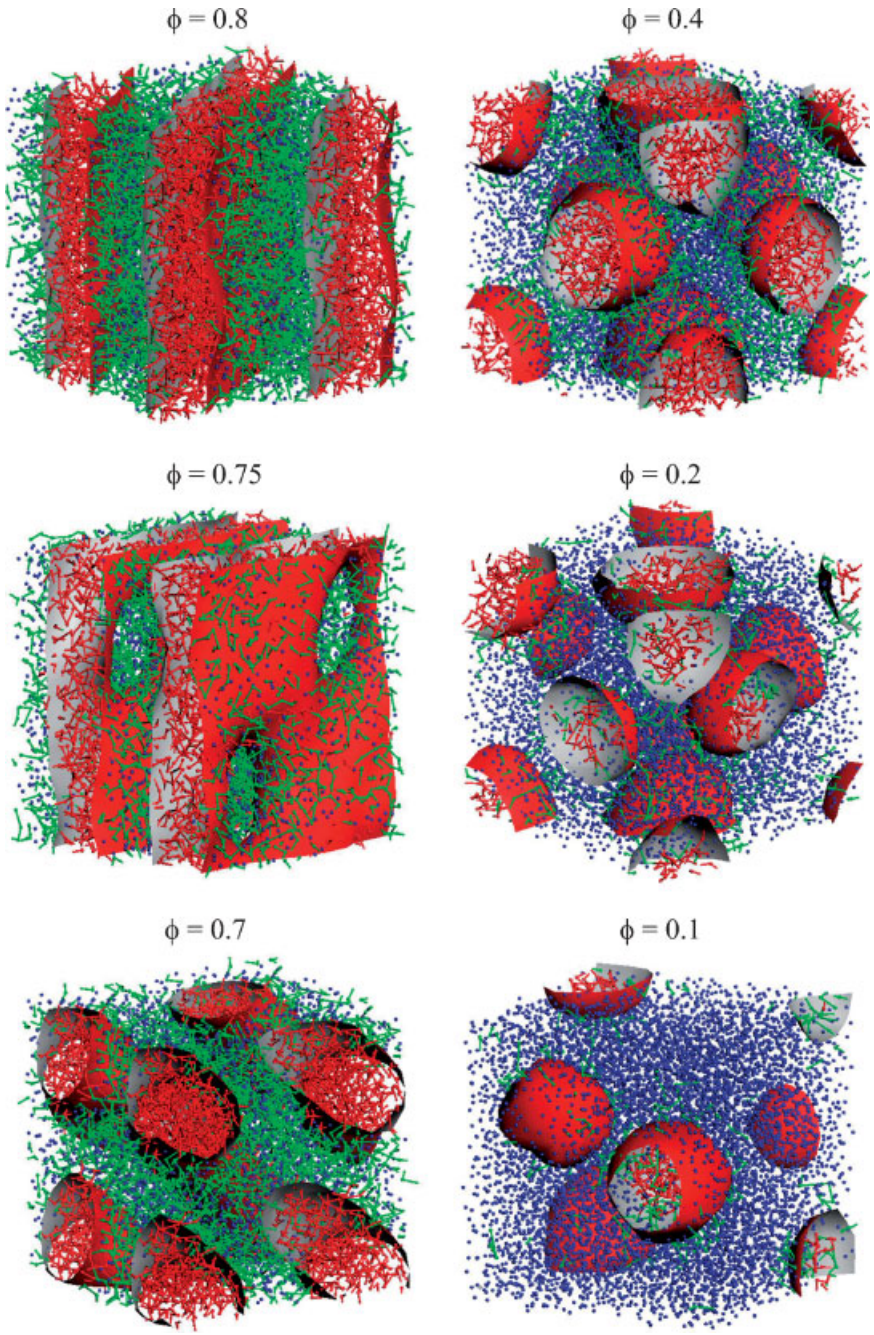

Figure 3. Morphology variation of A_5B_5 in the presence of a selective solvent S with ϕ, simulated in a box of $15 \times 15 \times 15$. The interaction parameters are set as $a_{AS} = 50$, $a_{BS} = 25$, and $a_{AB} = 50$. The red, green, and blue colors represent A, B, and S, respectively. In each pattern, the isosurface of the A component is also shown.

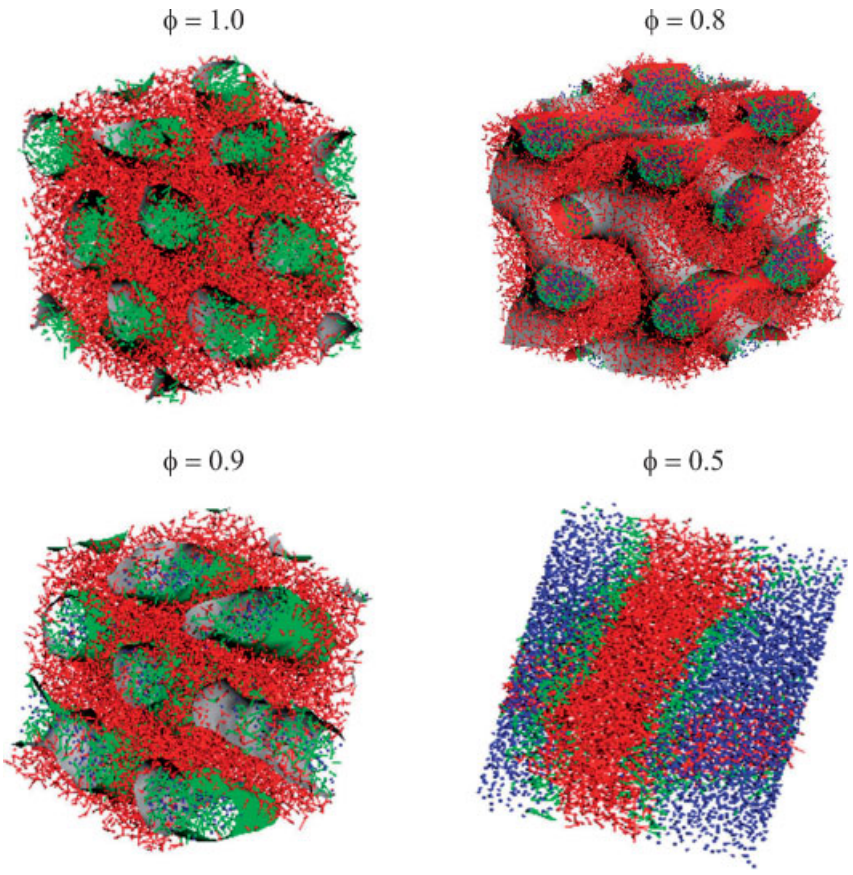

Figure 4. Morphology variation of A_8B_2 in the presence of a selective solvent S with ϕ. The interaction parameters are set as $a_{AS} = 50$, $a_{BS} = 25$, and $a_{AB} = 50$. All patterns are generated in a box of $15 \times 15 \times 15$, except the one at $\phi = 0.8$, generated in a box of $20 \times 20 \times 20$. The red, green, and blue colors represent A, B, and S, respectively. The red and green surfaces correspond to the isosurfaces of A and B, respectively.

of $C_B^{HEX}(1.0 \geq \phi \geq 0.9) \rightarrow G_B \quad (\phi = 0.8) \rightarrow$ 2-macrophase ($\phi \leq 0.7$) occurs. In general, these DPD simulated results have been in a qualitatively good agreement with our previous SCMF results except for the spherical ordering phase.[34] Recall that both experimental[13,26] and theoretical[34] studies have confirmed that the formed "normal" spheres adopt a bcc lattice while the "inverted" spheres tend to pack from bcc to fcc upon increasing the solvent selectivity and/or solvent amount. However, our DPD results for the systems in Figure 2 demonstrate that the formed spheres when $f = \approx 0.4$–0.6 and ≈ 0.2–0.3 adopt the packing array of fcc and A15, respectively. In Figure 3 and Figure 5 we present the typical fcc and A15 packed spheres formed by A_5B_5 ($f = 0.5$) and A_3B_7 ($f = 0.3$), respectively, at $\phi = 0.4$, $a_{AS} = 50$, $a_{BS} = 25$, and $a_{AB} = 50$. With a further inspection, the number of the effective spheres formed within the same simulation box of $15 \times 15 \times 15$ in Figure 3 and 5 is equal to 4 and 8, respectively, which simply corresponds to the value of effective spheres in a fcc and A15 lattice, respectively. In our previous DPD study of phase behavior of A_1B_3 amphiphilic molecules in two solvents, we observed various spherical packing orders, such as bcc, fcc, and A15, by simulating the same system but with different box sizes.[49] Though we did not perform the simulations with different box sizes here, we believe that this finite size effect on the spherical packing order also exists in the diblock copolymer solutions when only one solvent is added. However, for the lamellar and hexagonally packed cylindrical phases, as long as the simulation box size is significantly larger than the radius of gyration of amphiphilic molecules, we observe no finite size effects as in the spherical phase via DPD. Generally speaking, though DPD may not identify the most stable packing array of spheres due to the significant finite size effects, it reveals the possibility for the spheres packing into an A15 lattice, which has been ignored in previous SCMF studies. Indeed, in addition to fcc and bcc, A15 has been proposed a quite possible state in the amphiphilic molecule systems.[50] To compare the difference between these spherical ordered phases experimentally, small-angle X-ray scattering (SAXS) is frequently employed, as the allowed reflection peaks occur at

Macromol. Theory Simul. **2007**, *16*, 77–85

Macromolecular Journals
DOI: 10.1002/mats.200600057

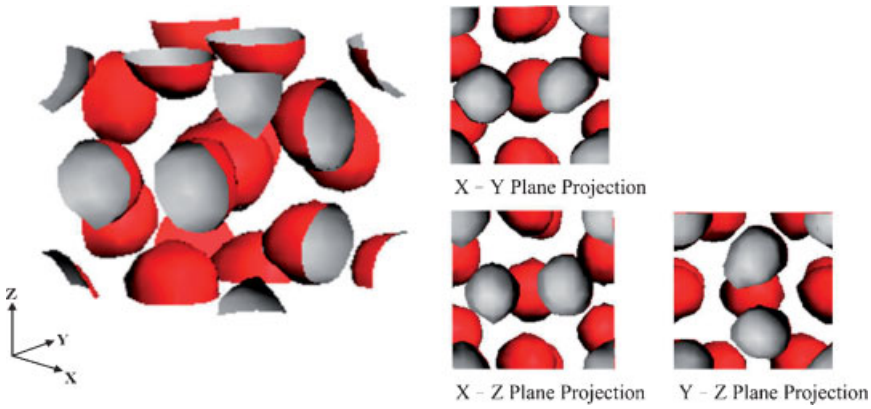

Figure 5. Morphology patterns of A_3B_7 in the presence of a selective solvent S with $\phi = 0.4$, $a_{AS} = 50$, $a_{BS} = 25$, and $a_{AB} = 50$, simulated in a box of $15 \times 15 \times 15$. In each pattern, only the isosurface of A component is shown.

$\sqrt{2} : \sqrt{4} : \sqrt{6} : \sqrt{8} : \sqrt{10} \ldots$, $\sqrt{3} : \sqrt{4} : \sqrt{8} : \sqrt{11} : \sqrt{12} \ldots$, and $\sqrt{4} : \sqrt{5} : \sqrt{6} : \sqrt{12} : \sqrt{13} \ldots$, for bcc, fcc, and A15, respectively.

To examine the effects of solvent selectivity and ϕ on the resulting phase behavior by DPD, we set a_{BS} equal to 25 and vary a_{AS}. Figure 6 presents the resulting phase map as a function of ϕ and a_{AS} for symmetric amphiphilic molecules A_5B_5 when $a_{AB} = 50$. As expected, the ordered regime is greatly enlarged with the solvent selectivity. When the solvent is neutral ($a_{AS} = a_{BS} = 25$), a transition of $L \rightarrow D$ occurs upon dilution. When a slightly selective solvent is added, a sequence from $L \rightarrow PL_A \rightarrow C_A^{HEX} \rightarrow D^{micelle} \rightarrow D$ is observed with decreasing ϕ. Increasing the solvent selectivity enables these spheres formed at $\phi \approx 0.2$–0.4 to adopt an ordered array. In addition, as the solvent selectivity increases, more solvent is expelled from the A-formed cores into the matrix regimes. Accordingly, the overlapping degree of B-chains in the matrix decreases upon increasing the solvent selectivity, as shown in Figure 7 where we present the spherical patterns formed by the symmetric A_5B_5 in a B-selective solvent with $\phi = 0.4$ and $a_{BS} = 25$ at various values of a_{AS}. As has been observed in both experimental[13,26] and SCMF theoretical[34] studies, when the solvent selectivity is slight, due to the fact that the chain overlapping degree is larger, the formed spheres have long-range interactions like the soft

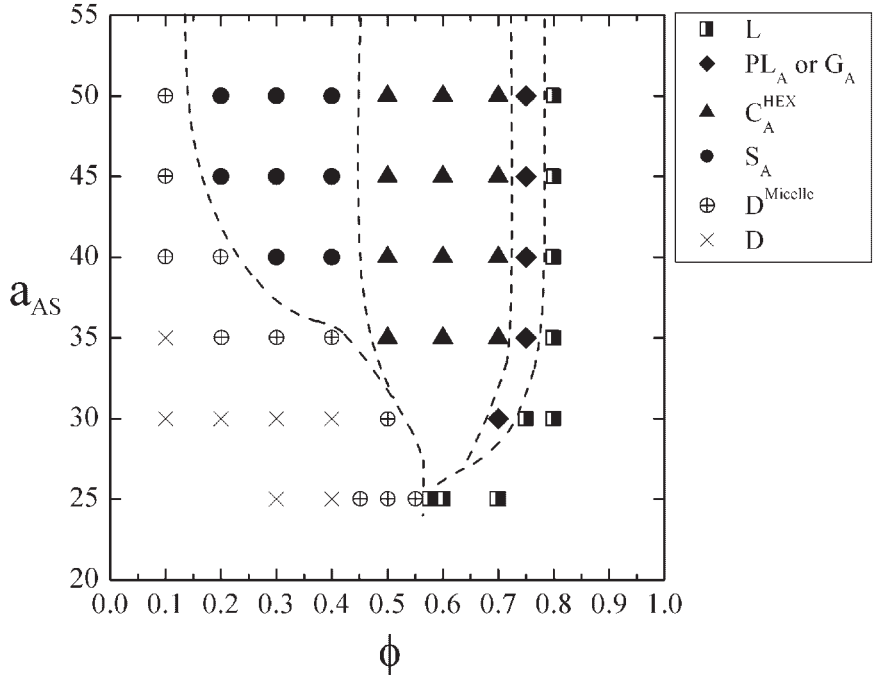

Figure 6. Two-dimensional phase map as a function of ϕ and a_{AS} for a symmetric amphiphilic molecule A_5B_5 in the presence of a solvent when $a_{AB} = 50$ and $a_{BS} = 25$.

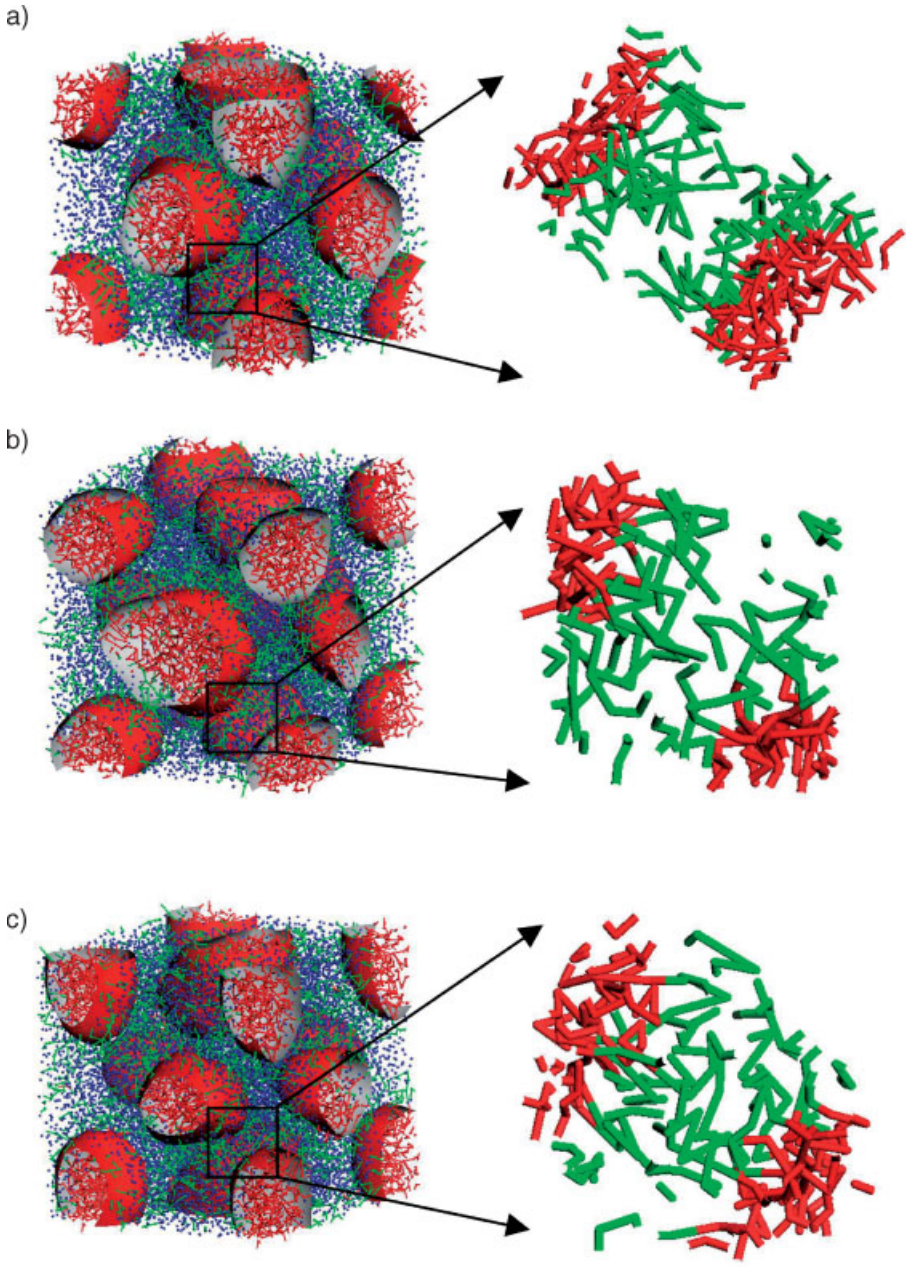

Figure 7. Spherical patterns formed by symmetric A_5B_5 in a B-selective solvent simulated in a box of $15 \times 15 \times 15$ with $\phi = 0.4$, $a_{AB} = 50$, $a_{BS} = 25$, and $a_{AS} =$ (a) 50, (b) 45, and (c) 40, respectively. The red, green, and blue colors represent A, B, and S, respectively. In each pattern, the isosurface of A component is also shown.

spheres and thus may adopt a less dense bcc packing; upon increasing the solvent selectivity, the decrease in the chain overlapping degree enables these spheres to adopt a more dense fcc packing like the hard spheres.

Conclusion

We employ DPD to simulate the phase behavior of an AB type of short amphiphilic molecules in the presence of one solvent S. In particular, the effects of composition of amphiphilic molecules, solvent selectivity, and solvent amount, are examined. In the neutral good solvents, our current DPD results reveal that the symmetric amphiphilic molecules undergo a lyotropic transition from a well ordered lamellar to a micelle-like and then to a totally disordered phase, which is analogous to the thermotropic transition in the melts. Indeed, for neutral good solvents the order-disorder transition results via the DPD are in good agreement with the theoretical predictions by

Macromol. Theory Simul. **2007**, *16*, 77–85

Macromolecular Journals
DOI: 10.1002/mats.200600057

including fluctuation effects as well as with experimental studies. In the selective solvents, DPD has successfully captured most of the phase transition behavior obtained by both SCMF calculations and experiments. For example, various transitions from the "normal" phases (i.e., the minority blocks form the minor domains) to even the "inverted" phases (formed by the majority blocks) can be induced by varying solvent selectivity and solvent amount. Furthermore, for the inverted spherical phase the chain overlapping degree in the matrix decreases with the solvent selectivity, which has also been observed in the thermotropic transition of bcc → fcc by the SCMF theory. Though the packing order of the spherical micelles is greatly affected by the finite size of the simulation box, DPD reveals a possible order of A15, which has been ignored in current SCMF work.

Acknowledgements: This work was supported by the *National Science Council of the Republic of China* through grant NSC 94-2216-E-002-027.

Received: August 9, 2006; Revised: September 21, 2006; Accepted: September 22, 2006; DOI: 10.1002/mats.200600057

Keywords: amphiphiles; dissipative particle dynamics; phase behavior; solvent selectivity

[1] O. G. Mouritsen, "*Life-As a Matter of Fat: The Emerging Science of Lipidomics Series*", Springer, New York 2005.
[2] N. Garti, A. Spernath, A. Aserin, R. Lutz, *Soft Matter* **2005**, *1,* 206.
[3] "*Developments in Block Copolymer Science and Technology*", I. W. Hamley, Ed., Wiley, New Jersey 2004.
[4] N. Hadjichristidis, S. Pispas, G. Floudas, "*Block Copolymers: Synthetic Strategies, Physical Properties, and Applications*", Wiley, New Jersey 2003.
[5] T. P. Lodge, *Macromol. Chem. Phys.* **2003**, *204,* 265.
[6] "*Amphiphilic Block Copolymers: Self-Assembly and Applications*", P. Alexandridis, B. Lindman, Eds., Elsevier, New York 2000.
[7] E. Helfand, Y. Tagami, *J. Chem. Phys.* **1972**, *56,* 3592.
[8] K. M. Hong, J. Noolandi, *Macromolecules* **1983**, *16,* 1083.
[9] M. D. Whitmore, J. Noolandi, *J. Chem. Phys.* **1990**, *93,* 2946.
[10] M. D. Whitmore, J. D. Vavasour, *Macromolecules* **1992**, *25,* 2041.
[11] C. I. Huang, T. P. Lodge, *Macromolecules* **1998**, *31,* 3556.
[12] K. J. Hanley, T. P. Lodge, *J. Polym. Sci. B* **1998**, *36,* 3101.
[13] K. J. Hanley, T. P. Lodge, C. I. Huang, *Macromolecules* **2000**, *33,* 5918.
[14] T. P. Lodge, K. J. Hanley, B. Pudol, V. Alahapperuma, *Macromolecules* **2003**, *36,* 816.
[15] M. Olvera de la Cruz, *J. Chem. Phys.* **1989**, *90,* 1995.
[16] G. H. Fredrickson, L. Leibler, *Macromolecules* **1989**, *22,* 1238.
[17] T. P. Lodge, C. Pan, X. Jin, Z. Liu, J. Zhao, W. W. Maurer, F. S. Bates, *J. Polym. Sci. B* **1995**, *33,* 2289.
[18] H. Watanabe, T. Kotaka, T. Hashimoto, M. Shibayama, H. Kawai, *J. Rheol.* **1982**, *26,* 153.
[19] M. Shibayama, T. Hashimoto, H. Kawai, *Macromolecules* **1983**, *16,* 16.
[20] G. A. McConnell, A. P. Gast, J. S. Huang, S. D. Smith, *Phys. Rev. Lett.* **1993**, *71,* 2102.
[21] G. A. McConnell, M. Y. Lin, A. P. Gast, *Macromolecules* **1995**, *28,* 6754.
[22] G. A. McConnell, A. P. Gast, *Phys. Rev. E* **1996**, *54,* 5447.
[23] G. A. McConnell, A. P. Gast, *Macromolecules* **1997**, *30,* 435.
[24] J. A. Pople, I. W. Hamley, J. P. A. Fairclough, A. J. Ryan, B. U. Komanschek, A. J. Gleeson, G. E. Yu, C. J. Booth, *Macromolecules* **1997**, *30,* 5721.
[25] I. W. Hamley, J. A. Pople, O. Diat, *Colloid. Polym. Sci.* **1998**, *276,* 446.
[26] T. P. Lodge, B. Pudil, K. J. Hanley, *Macromolecules* **2002**, *35,* 4707.
[27] J. Bang, T. P. Lodge, X. Wang, K. L. Brinker, W. R. Burghardt, *Phys. Rev. Lett.* **2002**, *89,* 215505.
[28] J. Bang, T. P. Lodge, *J. Phys. Chem. B* **2003**, *107,* 12071.
[29] M. J. Park, J. Bang, T. Harada, K. Char, T. P. Lodge, *Macromolecules* **2004**, *37,* 9064.
[30] C. Lai, W. B. Russel, R. A. Register, *Macromolecules* **2002**, *35,* 841.
[31] C. Lai, W. B. Russel, R. A. Register, *Macromolecules* **2002**, *35,* 4044.
[32] M. Banaszak, M. D. Whitmore, *Macromolecules* **1992**, *25,* 3046.
[33] J. Noolandi, A. C. Shi, P. Linse, *Macromolecules* **1996**, *29,* 5907.
[34] C. I. Huang, H. Y. Hsueh, *Polymer* **2006**, *47,* 6843.
[35] P. Hoogerbrugge, J. Koelman, *Europhys. Lett.* **1992**, *19,* 155.
[36] R. D. Groot, P. B. Warren, *J. Chem. Phys.* **1997**, *107,* 4423.
[37] R. D. Groot, T. J. Madden, *J. Chem. Phys.* **1998**, *108,* 8713.
[38] S. Yamamoto, Y. Maruyama, S. Hyodo, *J. Chem. Phys.* **2002**, *116,* 5842.
[39] E. Ryjkina, H. Kuhn, H. Rehage, F. Muller, J. Peggau, *Angew. Chem. Int. Ed.* **2002**, *41,* 983.
[40] L. Rekvig, M. Kranenburg, J. Vreede, B. Hafskjold, B. Smit, *Langmuir* **2003**, *19,* 8195.
[41] S. G. Schulz, H. Kuhn, G. Schmid, C. Mund, J. Venzmer, *Colloid. Polym. Sci.* **2004**, *283,* 284.
[42] R. D. Groot, *Lect. Notes Phys.* **2004**, *640,* 5.
[43] M. Y. Kuo, H. C. Yang, C. Y. Hua, C. L. Chen, S. Z. Mao, F. Deng, H. U. Wang, Y. R. Du, *Chem. Phys. Chem.* **2004**, *5,* 575.
[44] H. J. Qian, Z. Y. Lu, L. J. Chen, Z. S. Li, C. C. Sun, *Macromolecules* **2005**, *38,* 1395.
[45] X. Cao, G. Xu, Y. Li, Z. Zhang, *J. Phys. Chem. A* **2005**, *109,* 10418.
[46] M. W. Matsen, F. S. Bates, *Macromolecules* **1996**, *29,* 1091.
[47] P. Espanol, P. B. Warren, *Europhys. Lett.* **1995**, *30,* 191.
[48] M. P. Allen, D. J. Tildesley, "*Computer Simulation of Liquids*", Clarendon, Oxford 1987.
[49] C. I. Huang, Y. J. Chiou, Y. K. Lan, *Polymer* **2007**, in press.
[50] P. Ziherl, R. D. Kamien, *J. Phys. Chem. B* **2001**, *105,* 10147.